NeuroImage: Clinical 17 (2018) 835–846

Contents lists available at ScienceDirect

NeuroImage: Clinical

journal homepage: www.elsevier.com/locate/ynicl

Increased insula-putamen connectivity in X-linked dystonia-parkinsonism☆

Anne J. Blood[a,b,c,d,e,g,*,1], Jeff L. Waugh[a,c,e,f,g,1], Thomas F. Münte[h], Marcus Heldmann[h], Aloysius Domingo[i], Christine Klein[i], Hans C. Breiter[a,b,d,j], Lillian V. Lee[k], Raymond L. Rosales[k,l], Norbert Brüggemann[h,i,**]

[a] Mood and Motor Control Laboratory, Massachusetts General Hospital (MGH), Charlestown, MA, USA
[b] Laboratory of Neuroimaging and Genetics, MGH, Charlestown, MA, USA
[c] Depts. of Neurology, MGH, Boston, MA, USA
[d] Psychiatry, MGH, Boston, MA, USA
[e] Martinos Center for Biomedical Imaging, Dept. of Radiology, MGH, Charlestown, MA, USA
[f] Division of Child Neurology, Boston Children's Hospital, USA
[g] Harvard Medical School, Boston, MA, USA
[h] Department of Neurology, University of Lübeck, Lübeck, Germany
[i] Institute of Neurogenetics, University of Lübeck, Lübeck, Germany
[j] Warren Wright Adolescent Center, Department of Psychiatry and Behavioral Sciences, Northwestern University Feinberg School of Medicine, Chicago, IL, USA
[k] XDP Study Group, Philippine Children's Medical Center, Quezon City, Philippines
[l] Department of Neurology and Psychiatry, Faculty of Medicine and Surgery, University of Santo Tomas, Manila, Philippines

ARTICLE INFO

Keywords:
Striosomes
Matrix
Paralimbic
Sensorimotor
Tractography

ABSTRACT

Preliminary evidence from postmortem studies of X-linked dystonia-parkinsonism (XDP) suggests tissue loss may occur first and/or most severely in the striatal striosome compartment, followed later by cell loss in the matrix compartment. However, little is known about how this relates to pathogenesis and pathophysiology. While MRI cannot visualize these striatal compartments directly in humans, differences in relative gradients of afferent cortical connectivity across compartments (weighted toward paralimbic versus sensorimotor cortex, respectively) can be used to infer potential selective loss in vivo. In the current study we evaluated relative connectivity of paralimbic versus sensorimotor cortex with the caudate and putamen in 17 individuals with XDP and 17 matched controls. Although caudate and putamen volumes were reduced in XDP, there were no significant reductions in either "matrix-weighted", or "striosome-weighted" connectivity. In fact, paralimbic connectivity with the putamen was elevated, rather than reduced, in XDP. This was driven most strongly by elevated putamen connectivity with the anterior insula. There was no relationship of these findings to disease duration or striatal volume, suggesting insula and/or paralimbic connectivity in XDP may develop abnormally and/or increase in the years before symptom onset.

1. Introduction

X-linked dystonia-parkinsonism (XDP) is a rapidly progressing disease that typically begins with severe dystonia and eventually combines with or is replaced by parkinsonism. It is seen almost exclusively in males, and most often manifests in the early to mid-thirties (Lee et al., 2001; Lee et al., 2011; Rosales, 2010). The disease reduces life expectancy of affected individuals, and involves substantial burden on both patients and caregivers. The disease is inherited in an X-linked recessive fashion, and genetic analyses of affected individuals, their relatives, and ethnically matched controls revealed seven disease-specific genetic alterations that segregate with disease (Domingo et al., 2015; Nolte et al., 2003). All are within introns of, or are in the region of the *TAF1* gene in the long arm of the X-chromosome. The underlying molecular genetic mechanisms, pathology, and pathophysiology XDP, however, are not completely understood (Makino et al., 2007; Nolte et al., 2003).

Critical clues to XDP disease mechanism(s) may be found by

☆ This study was conducted as part of the Collaborative Center for X-linked Dystonia-Parkinsonism (XDP) at Massachusetts General Hospital.

* For matters relating to study concept and tractography approach, correspondence should be addressed to: A.J. Blood, 120 2nd Avenue, Charlestown, MA 02129, USA.
** For matters relating to study oversight and clinical assessment, correspondence should be addressed to: N. Brüggemann, Institute of Neurogenetics, Department of Neurology, University of Lübeck, Lübeck, Germany.
E-mail addresses: ablood@nmr.mgh.harvard.edu (A.J. Blood), norbert.brueggemann@neuro.uni-luebeck.de (N. Brüggemann).

[1] Authors made equal contributions.

https://doi.org/10.1016/j.nicl.2017.10.025
Received 2 March 2017; Received in revised form 27 September 2017; Accepted 24 October 2017
Available online 28 October 2017

studying the location and characteristics of neural degeneration. Previous studies indicate that, unlike typical Parkinson Disease, cell loss in XDP takes place in the striatum, and not in the substantia nigra (Eidelberg et al., 1993; Goto et al., 2005; Lee et al., 2001; Waters et al., 1993). A SPECT study further corroborated structural imaging by showing that postsynaptic, rather than presynaptic dopaminergic tracer uptake in the striatum was reduced in XDP (Bruggemann et al., 2017). Within the striatum itself, a postmortem study found evidence in XDP for differential cell loss across two histochemically distinct compartments of the mammalian striatum: the striosomes and the matrix (Goto et al., 2005). Specifically, they found evidence for greater cell loss in the striosomes than the matrix. These two striatal compartments are anatomically indistinguishable by current neuroimaging techniques, but prior animal tract-tracing studies indicate the compartments exhibit distinct patterns of extra-striate connectivity suggesting highly segregated functional roles. Specifically, the greater weight toward paralimbic connectivity with striosomes suggests this compartment may provide a means by which emotion and behavior assist in driving motor function linked to the matrix. For example, a combined optogenetic and electrophysiology approach was used recently in rats to show that a medial prefronto-striosomal circuit was selectively active during and necessary for making cost-benefit decisions during approach-avoidance conflict (Friedman et al., 2015). In addition, lesions of the striosomes have been shown to reduce behavioral stereotypies that normally result from cocaine administration in rats (Murray et al., 2015). These findings are consistent with a hypothesis that striosome- or matrix-specific injury may underlie particular features of human disease (Crittenden and Graybiel, 2011). While this has not been directly tested in humans, some studies have indirectly tested this hypothesis based on evaluation of functions thought to be mediated by distinct basal ganglia loops [e.g., (Beste et al., 2010)].

The potential importance of striatal compartments to XDP is further underlined by the fact that dystonia is the predominant phenotype in the first phase of XDP, and is hypothesized to be due to striosomal loss and SNpc disinhibition, while parkinsonism usually occurs later and is hypothesized to be related to matrisomal loss (Goto et al., 2005). Therefore, further studies are needed to better understand the status of these two compartments in living individuals with XDP. In particular, postmortem studies are not capable of distinguishing between greater striosomal loss and insufficient development of striosomes from early life.

The striosome and matrix compartments differ in their connectivity with other brain regions in several ways, including: (1) only striosomes project to the substantia nigra pars compacta (SNc), and may modulate the amount of nigral input to both striatal compartments (Dure et al., 1992; Graybiel et al., 2000; Langer and Graybiel, 1989) and (2) cortical projections to striosomes are weighted toward limbic cortical regions (i.e., paralimbic cortex), whereas projections to the matrix are weighted toward primary sensory and motor cortical regions (Eblen and Graybiel, 1995; Gerfen, 1984, 1989; Jimenez-Castellanos and Graybiel, 1987; Kincaid and Wilson, 1996; Ragsdale and Graybiel, 1981). While most cortical regions project to both striosomes and matrix, the relative weighting of connections across primary, association, and limbic cortex projections differs between the two striatal compartments. Thus, striosomal loss might lead to both faulty modulation of motor output and dysregulation of limbic function, consistent with the psychiatric comorbidity often observed in XDP (Morigaki et al., 2013). However, it is unknown whether comorbidity is primary or secondary to the disease.

The challenge of characterizing the relative involvement of striosome versus matrix compartments in XDP is that current MRI methods do not allow detection of the striosome/matrix distinction (Crittenden and Graybiel, 2011), both because these compartments are not visible without immunohistochemical staining and because striosomes are small enough that even 7T structural MRI protocols have insufficient resolution to visualize them directly. However, because cortical connectivity is weighted differently between the two compartments, diffusion tensor imaging (DTI) tractography provides a method to test predictions from hypotheses about the relative integrity of these two regions. While an indirect approach, it is the best we have at this time, and it may also be used to generate new hypotheses about XDP that can allow for more targeted testing when postmortem brains become available.

DTI has been used extensively in the past to evaluate brain white matter integrity and connectivity in dystonia and Parkinson disease (Argyelan et al., 2009; Blood et al., 2012; Blood et al., 2006; Carbon et al., 2004; Delmaire et al., 2009; Hess et al., 2013). Although diffusion tractography is the best existing method for evaluating structural connectivity in living humans, it is an inferential, rather than direct measure of anatomy, so DTI studies must work around certain challenges. For example, tractography does not detect direction of projections and therefore striatonigral projections, the connectivity feature most distinct between the two compartments, cannot be dissociated from nigrostriatal projections. As an alternative—albeit less direct—approach, cortical projections to the striatum (Gerfen, 1984; Ragsdale and Graybiel, 1981) can be used in an effort to dissociate the integrity of striosome versus matrix compartments. While we cannot be certain that projections to the site of degeneration will be lost, it is highly likely that there will be at least some remodeling of circuitry in the event that projection targets are lost (Isacson and Sofroniew, 1992). If loss of striosomal tissue (Str) were greater than loss of matrix (Mat) tissue in XDP, we would predict that paralimbic connectivity ("striosome-weighted") would be reduced relative to controls, and that this reduction would be greater than any reduction observed in sensorimotor connectivity ("matrix-weighted"). While previous diffusion tensor imaging studies in XDP suggested there are widespread differences in white matter diffusivity in XDP (Bruggemann et al., 2016), it is not known whether this finding reflected connectivity changes specific to the striatum or to one compartment or the other. To investigate this, tractography studies are needed.

In the current study we tested the hypothesis that paralimbic connectivity (striosome-weighted) would be reduced relative to controls, and that this reduction would be greater than any reduction observed in sensorimotor connectivity (matrix-weighted). Specifically, we evaluated probabilistic tractography between several striosome-weighted (anterior insula, anterior/subcallosal cingulate, and orbitofrontal cortex), and matrix-weighted (primary motor, primary somatosensory, dorsolateral premotor, and supplementary motor area) cortical regions and striatal nuclei in 17 Filipino XDP patients with a range of disease severity and compared these individuals with 17 matched Filipino control subjects. Because the striosome/matrix difference in tissue loss was hypothesized to be greatest early in the disease (Goto et al., 2005) we evaluated individuals who had been symptomatic from one to six years.

2. Materials and methods

2.1. Participants

17 Filipino XDP patients and 17 age, sex, handedness, and race-matched controls (see Table 1 and *XDP/control cohort matching* below) were scanned as part of a multimodal imaging study at the University of Lübeck. As noted in Table 1 and Supplementary Table 1 in Appendix I), we also evaluated findings in two smaller cohorts with complementary demographic matching approaches (described further below in XDP/control cohorts and matching). The control group consisted of unaffected relatives of the XDP patients (n = 6) and subjects recruited by advertisement (n = 11). Patients were recruited by the Philippine XDP study group in collaboration with the Institute of Neurogenetics, University of Lübeck, Germany. The patients were referred to the University of Lübeck to undergo pallidal deep brain stimulation (DBS) for severe and treatment-refractory XDP. Prior to DBS, the patients were

Table 1
Demographic characteristics of XDP and Control cohorts.

		XDP patients	Controls	*statistic(p)
17 XDP vs. 17 controls	Age	40.5 ± 8.2 y	37.2 ± 7.9 y	F = 1.420(0.242)
	Sex (male/female)	16/1	15/2	χ^2 = 0.366(0.500)
	Handedness (R/L/Ambidex)	15/1/1	16/0/1	χ^2 = 1.032(0.597)
	Scanner (Achieva/Ingenia)	13/4	16/1	χ^2 = 0.211(0.168)
	Age at onset (range)	36.6 ± 7.2 y (29–49)		
	BFM-M total (range)	51.3 ± 23.1 (3.5–88)		
	BFM-M speech (range)	7.3 ± 5.5 (0–16)		
	UPDRS-III total (range)	37.6** ± 16.4 (5–62)		
	HADS-D (range, n)	5.9 ± 2.2 (3–9, 8)		
	HADS-A (range, n)	(7.7 ± 3.5 (1–12, 7)		
10 XDP vs. 10 controls	Age	39.5 ± 6.5 y	38.8 ± 7.7 y	F = 0.048(0.829)
	Sex (male/female)	10/0	10/0	
	Handedness (R/L/Ambidex)	8/1/1	9/0/1	χ^2 = 1.059(0.589)
	Scanner (Achieva/Ingenia)	10/0	10/0	
	Age at onset (range)	36.3 ± 6.6 y (29–48)		
	BFM-M total (range)	45.4 ± 25.3 (3.5–81)		
	BFM-M speech (range)	7.8 ± 6.2 (0–16)		
	UPDRS-III total (range)	33.9 ± 18.1 (5–62)		
	HADS-D (range, n)	5.8 ± 2.3 (3–9, 6)		
	HADS-A (range, n)	8.0 ± 4.2 (1–12, 5)		

XDP: X-linked dystonia-parkinsonism.
*For categorical variables we used Chi-Square tests and for continuous variables we used ANOVAs. No statistics were performed for variables that matched 100% between groups.
**Please see Methods Section 2.2 regarding the effects of dystonia symptoms on UPDRS scores. The patients in this study scored high primarily due to severe dystonia.

asked to voluntarily participate in a multimodal neuroimaging study. In five patients, head movements were too severe to acquire high quality magnetic resonance imaging (MRI) data under regular conditions. These patients were asked whether they would allow an additional MRI research scan to be done on the day of surgery when preoperative stereotactic planning MRI was performed. During this scan, patients were under general anesthesia. At this time point, the stereotactic frame used for surgery was already fixed on their heads but did not influence data quality, i.e. did not give rise to artifacts.

XDP patients were confirmed to carry disease-specific genetic alterations and all controls were confirmed to carry wild-type alleles. Alleles were determined using either PCR-based detection of a large insertion within the XDP linked region, or Sanger sequencing of single-nucleotide genetic alterations, as previously described (Domingo et al., 2015). XDP disease duration ranged from 1 to 6 years (Table 1). Most patients were in the dystonic phase, i.e. they mostly suffered from generalized dystonia, but there were also patients with clear parkinsonian symptoms (Table 1). Please see the note below in “Movement Disorder scales” regarding the difficulty of distinguishing between dystonic and parkinsonian symptoms using standard Parkinson scale scores.

2.1.1. Ethics statement

All participants included in this study signed written informed consent prior to participation in the study, and the study was approved by the Institutional Review Board of the University of Lübeck. All experiments were conducted in accordance with the principles of the Declaration of Helsinki.

2.1.2. XDP/control cohorts and matching

Subjects included in the current study were drawn from a total of 19 symptomatic patients and 24 controls with DTI data, to maximize the balance of demographic matching and cohort size. The main cohort was composed of 17 XDP patients and 17 matched healthy controls. Matching between cohorts was done at the group level for age, sex, handedness, and scanner (see Table 1 and below), and demographic and scanner characteristics were not significantly different across cohorts (Table 1). One symptomatic female XDP patient was included in this main cohort, along with two female control subjects. The woman with XDP had mild to moderate parkinsonism but not dystonia, a later age at onset, and a different genetic pattern in that she was homozygous for two mutated alleles. In this cohort, 13/17 XDP patients were scanned on a Philips Achieva 3.0T MR scanner, while the remaining four XDP patients were scanned on a Philips Ingenia 3.0T MR scanner, due to a change of magnet late in the study. 16/17 controls were scanned on the Achieva scanner, and one on the Ingenia scanner. Although scanner proportions did not differ significantly between groups (Table 1), we added a level of rigor by comparing data from the 17 vs.17 cohort against a smaller cohort of 10 XDP versus 10 controls for which both scanner and sex were perfectly (one-to-one) matched (all scanned on the Achieva magnet, all males), and age matching was tighter (Table 1). This cohort was a subset of subjects from the 17vs.17 cohort. We also evaluated a larger cohort matched one-to-one for scanner, but which was less well matched by sex than the other two cohorts (race matching was prioritized over sex matching for the new scanner), and similarly matched for age as the 17 versus 17 cohort; a description of and data from this third cohort can be found in Appendix I. Comparing across these three cohort combinations strengthens our arguments that findings relate to the disease, independent of demographic or scanner factors.

2.2. Clinical variables evaluated

2.2.1. Movement disorder scales

The Burke Fahn Marsden Rating Scale-movement (BFM-M) was used to evaluate dystonia symptoms in XDP and the Unified Parkinson's Disease Rating Scale part III (UPDRS-III) was used to evaluate parkinsonian symptoms. Note that the UPDRS-III scoring categories may capture more general features that may result from dystonia, leading to “false positives” in estimation of parkinsonian symptoms. The patient population studied here showed increased UPDRS scores mainly driven by severe dystonia. We observed, for example, impaired motor control, slowness of movements and ‘stiffness’ which is why most patients scored so high on the UPDRS even though they exhibited primarily dystonic symptoms. We did not ‘subtract’ dystonia which lessens the specificity of the UPDRS-III to detect Parkinsonian signs. These scales are usually used in separate patient populations and therefore do not usually encounter this issue. However, this underlines the need for improved or alternate scales to better distinguish these two types of symptoms for cases where there is overlap.

2.2.2. Mood disorder scales

The Filipino version of the Hospital Anxiety and Depression Scale (HADS) was used to evaluate depression and anxiety symptoms in XDP. This scale was used because of its availability translated into Tagalog/Pilipino, the national language of the Philippines most likely to be understood by the Filipino population regardless of their island of residence. HADS scores were available only for eight of the 17 XDP patients as the remaining nine of them were unable to complete these scales, due to motor impairment or general exhaustion.

2.2.3. Duration of disease

Duration of disease was measured as time from symptom onset via patient self-report.

2.3. Experimental design

2.3.1. Scanning protocol

Diffusion-weighted MRI data were recorded using a 32-direction DTI sequence (32-channel head coil, 70 slices, $2 \times 2 \times 2\,mm^3$ voxel size, $1000\,s/mm^2$, TR = 7582 ms, TE = 60 ms). To increase signal to noise ratio data were upsampled to an individual MPRAGE T1 image (200 slices, $1\,mm^3$ isometric).

2.3.2. DTI preprocessing

DTI images were preprocessed with standard FSL FMRIB software (Release 5.0, Sept. 2012, http://fsl.fmrib.ox.ac.uk/fsl/fslwiki), and components of FMRIB's Diffusion Toolbox using standard parameters. Specifically, we used FMRIB's Diffusion Toolbox (FDT v2.0). The initial data preprocessing for each subject included radiological orientation, removal of non-brain tissue (*BET*), and correction for head motion and eddy current distortions. *DTIFIT* reconstruction of diffusion tensors at each voxel was applied to create 3D images at the same matrix size and resolution as the original diffusion images, including fractional anisotropy (FA) maps for each subject.

Registration matrices were computed for each subject to register tractography seed, exclusion, and endpoint masks from MNI space into native space. Specifically, the FSL non-linear transform (*FNIRT*) was used to register native space FA images to the FMRIB58_FA_1mm brain (in same space as the MNI152_T1_1mm brain), and the inverse transform was computed for MNI-to-native space registration.

2.3.3. Probabilistic Tractography

2.3.3.1. General tractography parameters and methods. For tractography, we used the *probtrackx* utility from the FMRIB Diffusion Toolbox. Tractography was run in native space, using 50,000 iterations; given the relatively small cohort size, we increased the number of iterations relative to the default (5000) to boost signal-to-noise ratio. Because distance artificially affects tractography measures (e.g., (Taljan et al., 2011)) and the tracts investigated differed amongst each other in length, we used the distance correction algorithm in the FDT toolbox to minimize the likelihood of distance artifacts in tractography data.

We used a "termination" approach to evaluate probability of cortical connectivity with caudate and putamen, in which tractography stops after it reaches the outside layer of voxels at the endpoint region. We used this approach rather than using striatal nuclei as "waypoints" (in which projections go through the nucleus), due to the likelihood that cell loss within the striatal nuclei in XDP would lead to methodological confounds once entering the nucleus itself. Although tractography is less affected by density and orientation of surrounding tissue than FA, it is not completely immune to it (Behrens et al., 2007).

Each tractography measure was made as the total number of streamlines reaching the caudate or putamen; note that this is a unitless, probabilistic measure derived from the *probtrackx* algorithm and does not reflect number of individual tracts or axons. Because tractography was used as a surrogate for detecting compartment-specific tissue loss, we did not normalize for striatal volume in our primary analyses, as this would have removed the very effect we were trying to detect. That is, such normalization would have computed relative density of streamlines per voxel, but lost information about total number of streamlines across the nucleus, our measure of interest. However, we did test if there was a relationship between striatal volume and tractography (see Data analyses), to ask whether tractography findings were driven by volume loss, as predicted.

In addition, we considered that overall variance in head size (intracranial volume, or ICV) might add potential "nuisance" variance to volume-related measures. To remove head-size related contributions to tractography, we ran parallel analyses (see Data analyses) normalizing each tractography measure by ICV. ICV was computed using the eTIV (estimated total incracranial volume) feature of the Freesurfer recon-all step (www.freesurfer.net/fswiki/eTIV). It is highly debated whether such normalization is preferable to raw, unnormalized data. While in theory such normalization should reduce variance, in some cases it may inject even more variance, particularly for small brain structures (Arndt et al., 1991; Voevodskaya et al., 2014). Many volumetry studies now provide both volume-normalized and volume-unnormalized data so both approaches can be evaluated for similarity and consistency [e.g., (Waugh et al., 2016)].

2.3.3.2. Tractography seeds, endpoints, exclusion masks

Tractography masks were created in each subject's native space using a within-modality (DTI) registration of a standard space mask template since this is more accurate and consistent across subjects than registering structural segmentations from native T1 structural space to DTI space. Specifically, a standard space template for each seed and endpoint mask was adapted from ICBM152 brain segmentations done by the Center for Morphometric Analysis (CMA) for the MGH Phenotype Genotype Project in Addiction and Mood Disorders (PGP), using landmarks as described in (Gasic et al., 2009; Makris et al., 2008). Because the ICBM152 brain was a different resolution (2 mm) than the 1 mm template we used here (MNI152_T1_1mm brain), we smoothed and/or otherwise corrected the edges of these segmentations to fit the MNI152_T1_1mm brain and cross-checked with the FMRIB58_FA_1mm brain and atlas landmarks to assure an accurate anatomical fit (Supplementary Figs. 1–4, Appendix II)). For the regions segmented, there were no misalignments between the T1 and FA templates so no adjustments were made to the MNI T1 template masks. These mask templates in standard space were then registered to each subject's native DTI space, to serve as individual tractography masks, using the FA map transform matrices generated during DTI preprocessing (see DTI preprocessing above).

We visually inspected the native-space seed masks to confirm the accuracy of registration, particularly to be certain that registration was accurate in capturing the disproportionate decrease in volume in the striatal nuclei in XDP. While all masks were accurately registered within the confines of their gray and white matter boundaries, we noted that the medial border of the head of the caudate (adjacent to the lateral ventricle) was less accurate for patients than for controls. Specifically, while registration was accurate for the putamen, and for the body and tail of the caudate, registration failed to reflect the atrophy of the head of the caudate and incorporated many intraventricular voxels. We speculate that the non-linear registration tool we utililzed (*fnirt*) was less proficient at distinguishing between the voxels of the atrophied caudate and CSF than between caudate and white matter voxels, where it performed well in both patients and controls. To correct for this misregistration, we utilized the B0 diffusion scan as a mask to remove voxels occupying CSF space along the medial margin of the head of the caudate. We first normalized the B0 scan and removed all voxels below 15% amplitude. This isolated voxels that were within the lateral ventricles, and subtracting this mask from the caudate seed removed CSF contamination. This correction was applied identically for patients and controls.

Note that although we used termination tractography, endpoint

masks themselves included the entire caudate or putamen and reflected the native space volume of these nuclei; these masks were also used as the measure of caudate and putamen volumes in this study since the goal was to assess if there was a relationship between the expected reduction in mask volume and predicted reduction in connectivity to these nuclei. Given the unexpected elevation in tractography in XDP, we wanted to be sure that altered tractography did not simply reflect an error in registration/mask size; if masks turned out to be larger in patients (and/or if nuclei truly were larger in these patients) this could potentially account for the findings and would suggest we were not working with a representative XDP population. Please note that this part of our methods was not intended to be a volumetry study of these individuals.

Tractography was run in native space using pairs of seed and endpoint regions. Seed regions included (1) precentral sulcus and dorsolateral/medial regions of the precentral gyrus, including primary motor cortex and dorsolateral premotor cortex, (2) postcentral sulcus and gyrus, including somatosensory areas 3, 1, 2, (3) supplementary motor area, (4) orbitofrontal cortex [OFC], (5) anterior/subcallosal cingulate cortex [ACC], and (6) anterior insula [aIns], which included the anterior half of the insula. (1)–(3) were used as "matrix-weighted" regions (Supplementary Fig. 1) and (4)–(6) were used as "striosome-weighted" regions (Supplementary Fig. 2). Segmentations of the putamen and caudate nuclei were used as endpoints (Supplementary Fig. 3). Boundaries described for primary motor and premotor regions vary across the literature; the primary motor and dorsolateral premotor segmentation here was defined based on anatomical landmarks described in (Chouinard and Paus, 2006; Picard and Strick, 2001; White et al., 1997). Tractography was run separately for each cortical/striatal pairing. For all tractography, we used a segmentation of the entire thalamus as an exclusion mask to select for cortico-striatal, rather than striato-thalamo-cortical projections (Supplementary Fig. 4A,B), and a midline exclusion mask to prevent inter-hemispheric projections from contaminating ipsilateral projections of interest (Supplementary Fig. 4C,D).

2.3.4. Fractional anisotropy (FA) and mean diffusivity (MD) contrasts

We ran FA and MD contrasts for the 17 XDP versus 17 healthy controls cohort as a supplemental analysis to evaluate white matter integrity more generally in XDP, and as a complement to the analysis run by Brüggeman and colleagues (Bruggemann et al., 2016). Methods and Results/Discussion for this analysis are included as supplementary material in Appendix III.

2.4. Data analyses

Demographic statistics were run in SPSS; all other statistics were run using StatTools (Palisades Corporation, Ithaca, NY).

2.4.1. Comparison of striatal volume across XDP and controls

Before comparing tractography data, we evaluated caudate and putamen volume (using mask volumes from caudate and putamen segmentations), to verify that the XDP cohort showed the predicted reductions in striatal volume. We separately compared XDP versus control for (1) left caudate, (2) right caudate, (3) left putamen, and (4) right putamen using standard two-tailed *t*-tests, using both raw volumes and ICV-corrected volumes. Based on these four comparisons, we applied a corrected significance threshold of $p = 0.0125$, or $p = 0.05/4$. We also verified that cortical seed region volumes did not differ between XDP and controls ($p > 0.05$).

Finally, we checked whether ICV differed across XDP and control groups to ensure that head size did not affect group comparisons; for this negative control, we required that $p > 0.1$ to rule out group differences.

2.4.2. Striosome versus matrix-weighted tractography (a priori comparisons)

To test our main hypothesis that in XDP, striosome-weighted regions would show greater reductions in striatal connectivity than matrix-weighted regions, we calculated total number of streamline terminations at a given endpoint mask (across both hemispheres) for each cortical/striatal pair. We then averaged termination counts across: (1) the three striosome-weighted regions to caudate, (2) the three striosome-weighted regions to putamen, (3) the three matrix-weighted regions to caudate, and (4) the three matrix-weighted regions to putamen. We compared XDP to controls for each of these four measures using two-sample, two-tailed *t*-tests. We anticipated that we would see reductions in both striosome and matrix group comparisons, but there would be a greater reduction in striosome than matrix connectivity in XDP relative to controls. As mentioned above, we ran parallel t-tests with tractography normalized by ICV to remove potential variance due to overall head size.

2.4.3. Posthoc evaluation of individual pairs of regions

Once we evaluated overall group differences we looked at a subset of tractography to individual regions, since our results yielded an unexpected finding. Specifically, connectivity was increased, rather than decreased, between striosome-weighted regions and the putamen, which led us to ask whether this was driven by one cortical region and/or one hemisphere. For these posthoc analyses we again used two sample, two-tailed, t-tests to compare XDP versus controls for tractography (total number of streamlines) between each of the three striosome-weighted regions and the putamen. We evaluated left and right hemispheres separately, for a total of six comparisons (left OFC → Put, left ACC → Put, left aIns → Put, right OFC → Put, right ACC → Put, right aIns → Put). We also ran parallel t-tests using tractography normalized by ICV.

2.4.4. Corrections for multiple comparisons for tractography group contrasts

As outlined above, we made a total of 10 a priori and *posthoc* statistical group tractography comparisons (four a priori and 6 *posthoc*); correction for multiple comparisons used the Bonferroni approach with a significance threshold set to $p < 0.05/10$, or $p < 0.005$. Because supplemental t-test comparisons normalizing for ICV used the same tractography data as the t-tests and therefore were neither independent nor primary comparisons, we used the same correction threshold ($p < 0.005$) for these tests.

2.4.5. Negative control for insula findings

Diffusion imaging uses direction and distance of water diffusion to evaluate white matter integrity and connectivity. As a result, coherence—in addition to density of tracts—in a given region influences fractional anisotropy, and to a lesser extent, tractography (Behrens et al., 2007). Changes in one tract thus have the potential to affect DTI measures of other, crossing tracts (e.g., perpendicular tracts). In the current study, it was important to consider whether potential disease-related reductions in putaminal connectivity from descending sensorimotor fibers might have influenced tractography measures of crossing tracts. Specifically, sensorimotor and insular projections to the putamen run perpendicular to each other in the external and extreme capsules. To verify that the tractography signal for insula-putamen connectivity was not artificially boosted by reduced sensorimotor connectivity we ran the following negative control analysis: We ran a linear regression analysis across patients to assess the relationship between measures of (1) sensorimotor tractography to putamen (i.e., matrix-weighted), and (2) insula tractography to putamen. If sensorimotor reductions influenced insular tractography, we would expect to see an inverse (i.e., negative R^2) relationship between descending (matrix) and crossing (insula) connectivity. That is, the greater the reduction in descending (i.e., crossing) fibers, the higher the insula-putamen connectivity would

appear. The absence of an inverse relationship would support the interpretation that insula connectivity itself, rather than an artifact of other connectivity, was the driver of group differences. Since this was a negative control, we required that $p > 0.1$ to rule out an effect.

2.4.6. Evaluation of tractography in relation to XDP clinical variables and putaminal volume

We used linear regressions to evaluate the relationship of matrix-weighted tractography to (1) disease severity (BFM motor score for dystonia and UPDRS-III score for parkinsonism) and (2) disease duration. Note that dystonia can lead to "false positives" on the UPDRS-III scores and make it appear that patients exhibit parkinsonian symptoms when they are primarily dystonic (see Movement disorder scales in Section 2.2 above). This effect was further corroborated by the fact that BFM and UPDRS-III scores were highly correlated ($R2 = 0.54$), and was why we were not able to distinguish between connectivity effects relating to dystonia versus parkinsonian symptoms in our regressions.

We used linear regressions to evaluate the relationship of striosome-weighted tractography to (1) HADS depression score, (2) HADS anxiety score, and (3) disease duration. In addition, since the insula difference between groups was, unexpectedly, more salient than for the other two paralimbic regions, we evaluated relationships of clinical variables and volume measures to our main findings in the anterior insula, looking at: (1) the relationship of speech and mouth BFM sub-scores to left and right anterior insula connectivity with the putamen, and (2) the relationship of left/right putaminal volume to left/right anterior insula connectivity with the putamen, to determine if differences in connectivity were related to volume loss. Although these functions may be weighted more toward matrix, than striosomal, connectivity, we evaluated speech and mouth symptoms in relation to insula connectivity because the insula (including anterior insula) plays such a substantial role in these functions. This amounted to a total of 18 analyses; using a Bonferroni correction for multiple comparisons the significance threshold was $p = 0.05/18$, or 0.00278).

3. Results

3.1. Comparison of striatal volume across XDP and controls

Both caudate and putamen morphometric volumes were significantly reduced in XDP compared to healthy controls (Table 2). We confirmed that the female XDP patient showed volume reduction in line with the male patients; in fact, caudate and putamen volumes for this patient were below the XDP cohort average.

Table 2
Comparison of endpoint mask size across XDP and controls (striatal volume).

Region	XDP mean ± SD	Control mean ± SD	T-test [t (p)]
Left caudate			
Raw volume	1929 ± 648 mm^3	3021 ± 525 mm^3	−5.40(< 0.0001)*
ICV-corrected	0.000169	0.000265	−6.13(< 0.0001)*
Right caudate			
Raw volume	1967 ± 704 mm^3	3006 ± 500 mm^3	−4.96(< 0.0001)*
ICV-corrected	0.000171	0.000265	−5.54(< 0.0001)*
Left putamen			
Raw volume	2487 ± 607 mm^3	4520 ± 535 mm^3	−10.45(< 0.0001)*
ICV-corrected	0.000223	0.000399	−7.768(< 0.0001)*
Right putamen			
Raw volume	2271 ± 594 mm^3	4103 ± 460 mm^3	−10.05(< 0.0001)*
ICV-corrected	0.000204	0.000365	−7.782(< 0.0001)*

Negative t values indicate volume was reduced in XDP patients relative to control subjects.
XDP: X-linked dystonia-parkinsonism.
SD: standard deviation.
* Met significance criteria ($p < 0.0125$, [$p < 0.05$, corrected]).

None of the cortical seed region masks showed significantly different volume between XDP and controls (all $p > 0.05$).

Finally, there was no difference in ICV across groups (mean control = 1,432,143 ± 182,429 mm^3; mean XDP = 1,420,660 ± 181,866.74 mm^3; $t = -0.189$, $p = 0.851$)

3.2. Striosome versus matrix-weighted tractography (a priori comparisons)

For comparisons between the 17 XDP and 17 controls, the caudate showed no group differences for either striosome- or matrix-weighted connectivity (Table 3; Fig. 1A,C). The putamen showed significantly greater striosome-weighted connectivity in XDP patients (Table 3; Fig. 1B), but no group difference in matrix-weighted connectivity (Table 3; Fig. 1D). Mean differences were similar for the 10 XDP versus 10 controls cohort (Table 4; Fig. 2), although statistical power was reduced due to the smaller cohort size. Mean differences were also similar for the 16 XDP versus 16 controls cohort (Supplementary Table 2 in Appendix I; Supplementary Fig. 5). Results were similar for ICV normalized and un-normalized data.

3.3. Posthoc evaluation of tractography for individual seed-endpoint pairs

Further evaluation of individual regions/hemispheres between striosome-weighted cortex and putamen led to the following findings: all three cortical regions, including both hemispheres, showed higher mean connectivity in XDP patients in the 17 versus 17 cohort, except for left anterior/subcallosal cingulate, which showed a trend toward reduced connectivity with the putamen in XDP (Table 5; Fig. 3). Of the regions showing elevated connectivity, two were significant (left and right insula; Fig. 3A), and one reached trend level (left orbitofrontal cortex; Fig. 3C). Mean differences were similar for the 10 versus 10 cohort (Table 6; Fig. 4), although statistical power was reduced due to the small cohort size. Mean differences were also similar for the 16 XDP versus 16 controls cohort (Supplementary Table 3 in Appendix I; Supplementary Fig. 6). Results were similar for ICV normalized and un-normalized data.

3.4. Negative control for insula findings

There was no relationship between descending (sensorimotor) and crossing (insula) connectivity with the putamen across the 17 XDP patients (Fig. 3E). The R^2 for this correlation was positive (0.147), rather than negative, and the relationship was not statistically significant ($p = 0.128$).

Table 3
Striosome-weighted versus matrix-weighted tractography comparisons (17 XDP versus 17 matched controls).

Region	T-test [t (p)]	T-test [t (p)] using ICV-normalized tractography
Striosome-weighted (paralimbic) to caudate	−1.28 (0.212)	−1.42 (0.165)
Striosome-weighted (paralimbic) to putamen	3.82 (0.000600)*	3.68 (0.0008)*
Matrix-weighted (sensorimotor) to caudate	−0.110 (0.913)	0.0108 (0.991)
Matrix-weighted (sensorimotor) to putamen	−1.57 (0.125)	−1.64 (0.112)

Positive t values indicate tractography was elevated in XDP patients relative to control subjects; negative t values indicate tractography was reduced in XDP patients relative to control subjects.
XDP: X-linked dystonia-parkinsonism.
ICV: intracranial volume.
* Met significance criteria ($p < 0.005$, [$p < 0.05$, corrected]).

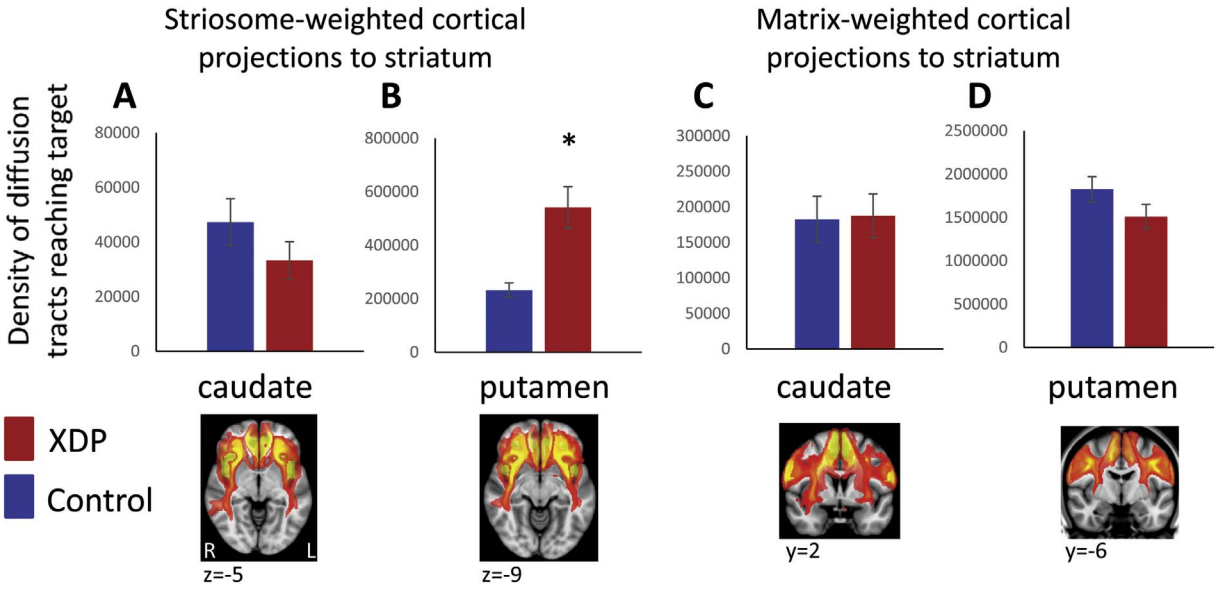

Fig. 1. Comparison of XDP versus control tractography for a priori comparisons. Total termination tractography counts are shown for the striosome-weighted and matrix-weighted regions for the caudate (A,C) and putamen (B,D). XDP values are shown in red and control values in blue. Error bars indicate standard error of the mean. XDP: X-linked dystonia-parkinsonism. Images (from *fslview*) below graphs show representative sections through the left and right hemisphere averaged healthy control tractography for each of the four a priori tractography measures, superimposed on the MNI152_T1_1mm template. Note that these images are intended (and thresholded) to be qualitative only, and are included simply to illustrate the territory covered most prominently by each of the four measures; they do not convey information about magnitude or spatial extent. The MNI coordinate indicates the location of each image slice. Images are in radiologic format; L: left hemisphere and R: right hemisphere. *significant at $p < 0.005$; †trend toward significance (within an order of magnitude of the significance p threshold).

Table 4
Striosome-weighted versus matrix-weighted tractography comparisons (10 XDP versus 10 matched controls).

Region	T-test [t (p)]	T-test [t (p)] using ICV-normalized tractography
Striosome-weighted (paralimbic) to caudate	−0.578 (0.571)	−0.396 (0.697)
Striosome-weighted (paralimbic) to putamen	2.79 (0.0122)†	3.15 (0.00550)†
Matrix-weighted (sensorimotor) to caudate	−0.541 (0.595)	0.759 (0.458)
Matrix-weighted (sensorimotor) to putamen	−1.701 (0.106)	−1.31 (0.207)

Positive t values indicate tractography was elevated in XDP patients relative to control subjects; negative t values indicate tractography was reduced in XDP patients relative to control subjects.
XDP: X-linked dystonia-parkinsonism.
ICV: intracranial volume.
† *p* value was within an order of magnitude of the corrected threshold (a trend).

3.5. Evaluation of tractography in relation to XDP clinical variables and putaminal volume

There was a trend toward significance in the relationship between left insula-putamen connectivity and the BFM mouth dystonia score in XDP patients (R = 0.538; p = 0.0316; Fig. 3D). No other clinical variables or volume measures showed relationships with tractography measures (all $p > 0.05$; for putamen volume/insula tractography correlations, left hemisphere: = 0.0978, p = 0.709; right hemisphere: R = 0.0482, p = 0.854).

3.6. Fractional anisotropy (FA) and mean diffusivity (MD) contrasts

Analysis of FA and MD in the 17 XDP versus 17 control cohort using TBSS indicated reduced FA and increased MD across much of the white matter skeleton in the XDP cohort, relative to healthy controls (Supplementary Fig. 7). Please see Appendix III for further details about this analysis.

4. Discussion

In this study, we failed to observe the predicted reduction in striatal connectivity with striosome-weighted cortical regions in XDP, despite substantial and significant reductions in caudate and putamen volume. Instead, we observed an unexpected elevation in striosome-weighted connectivity to the putamen. Mean striosome-weighted connectivity with putamen was more than twice the magnitude in XDP as in matched controls. Because this finding did not correlate with disease duration, it may reflect an “endophenotype” rather than the correlate of disease symptom expression or progression. Although our approach was not able to corroborate the hypothesized overweighting of striosomal depletion relative to matrix in XDP, it provided much-needed new clues about the pathology and pathophysiology of XDP that may lead us closer to the source of such depletion.

Specifically, increased striosome-weighted connectivity observed here in XDP suggests one or more of the following scenarios, which may or may not be specific to striosomes: (1) afferents are not lost when striatal tissue is lost, (2) there are white matter abnormalities in addition to striatal degeneration, (3) some disease-related plasticity and/or compensatory mechanism is taking place, and/or (4) connectivity with the putamen may have developed differently in XDP patients from an early age.

Scenario (1) suggested above seems unlikely, particularly since connectivity was substantially increased in XDP, rather than similar to controls. However, other changes might take place that boost the diffusion signal even with fewer afferents. For example, the diffusion signal is affected by factors such as myelination, in addition to number of axons (Beaulieu, 2002). This brings us to scenario (2).

Scenario (2) suggests there may be white matter abnormalities in XDP. It is particularly intriguing that XDP symptom onset occurs most typically near the age where regulation of myelination shifts from developmental to adult maintenance mechanisms (Breiter et al., 1994; Yakovlev and Lecours, 1982). This raises the possibility that myelination is normal in these individuals until it shifts to adult mechanisms, at

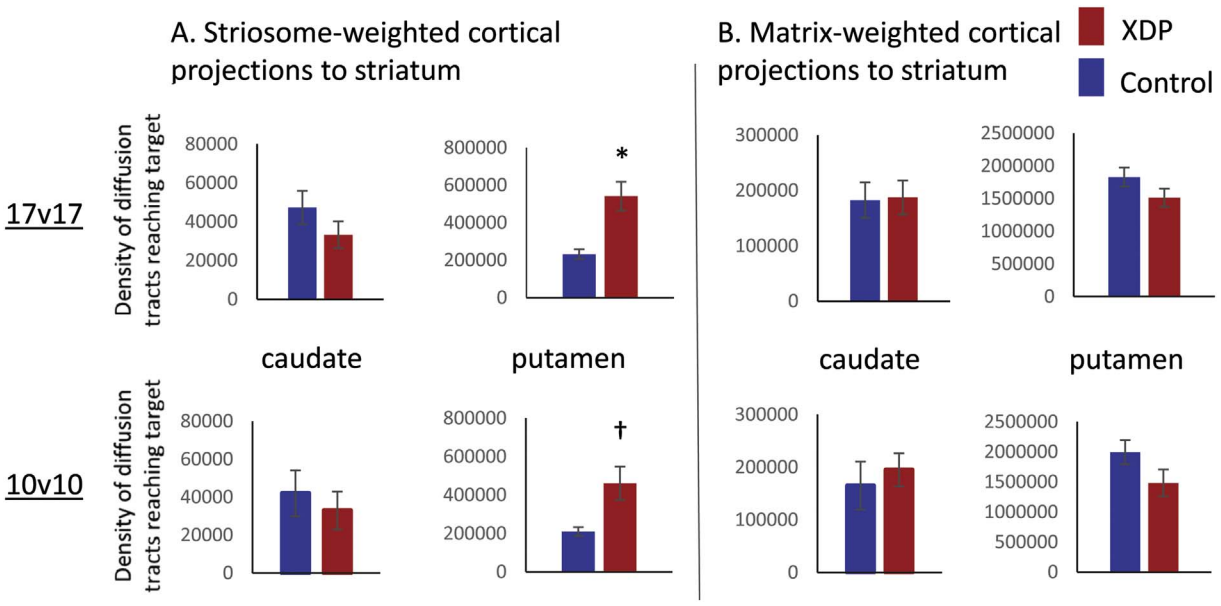

Fig. 2. Comparison of tractography measures for a priori comparisons in the 17 XDP versus 17 controls cohort, as compared with the 10 XDP versus 10 controls cohort. Total termination tractography counts from Fig. 1 (17 XDP versus 17 controls, top row) are compared with values for the smaller, more tightly matched cohort (bottom row). (A) Striosome-weighted region connectivity with the caudate (left) and putamen (right). (B) Matrix-weighted region connectivity with the caudate (left) and putamen (right). Error bars indicate standard error of the mean. *significant at $p < 0.005$; †trend toward significance (within an order of magnitude of the significance p threshold). XDP: X-linked dystonia-parkinsonism.

Table 5
Striosome-weighted tractography to putamen comparisons for individual regions (17 XDP versus 17 matched controls).

Region	T-test [t (p)]	T-test [t (p)] using ICV-normalized tractography
Left anterior insula to left putamen	3.05 (0.00450)*	2.89 (0.00690)†
Right anterior insula to right putamen	3.21 (0.00300)*	3.21 (0.00300)*
Left anterior/subcallosal cingulate to left putamen	−3.07 (0.00440)*	−3.30 (0.00240)*
Right anterior/subcallosal cingulate to right putamen	0.574 (0.570)	0.471 (0.641)
Left orbitofrontal cortex to left putamen	2.34 (0.0258)†	2.42 (0.0216)†
Right orbitofrontal cortex to right putamen	1.57 (0.127)	1.48 (0.149)

Top row values represent values not normalized for striatal volume; bottom rows ("Norm-to-vol" represent values after normalization for striatal volume (i.e., calculating density of connections per voxel, rather than absolute number of connections).
Positive t values indicate tractography was elevated in XDP patients relative to control subjects; negative t values indicate tractography was reduced in XDP patients relative to control subjects.
XDP: X-linked dystonia-parkinsonism.
ICV: intracranial volume.
* Met significance criteria ($p < 0.005$, [$p < 0.05$, corrected]).
† p value was within an order of magnitude of the corrected threshold (a trend).

which point regulation goes awry. This might be independent of the striatal degenerative process, or it might be a factor driving degeneration. A recent study in a subset of the patients and controls included here showed fairly global increases in mean diffusivity (MD) in XDP, despite only focal reductions in fractional anisotropy (FA) (Bruggemann et al., 2016). Supplementary analyses in the current study (Appendix III) show similar findings, albeit more widespread for both FA and MD, likely due to better power from the larger cohort. This finding is consistent with widespread axonal loss due to striatal degeneration but, alternatively, may reflect a more general white matter pathology in XDP. Since DTI is unable to distinguish between these two possibilities, future studies, including postmortem studies, should be conducted to evaluate white matter more directly in XDP. Recent work in adult white matter plasticity also suggests that DTI tractography measures may be influenced by activity-related factors affecting existing axons, effectively "highlighting" pathways that have substantially changed their level of function (Blood et al., 2006; Engvig et al., 2012; Lovden et al., 2010; Scholz et al., 2009; Ullen, 2009). Excessive brain function during symptom expression in XDP might increase the relative signal contribution of affected tracts, even if the total number of tracts is reduced.

Scenario (3)—the possibility of compensatory increases in connectivity—could have taken place either in response to medium spiny neuron depletion, or early in life if striosomal territory was reduced from development. The possibility of such compensatory mechanisms is consistent with a previous study showing that increased local volume (i.e., gray matter density) in the basal ganglia in asymptomatic individuals with Parkin and Pink1 mutations was inversely related to presynaptic striatal (18)F-DOPA uptake (Binkofski et al., 2007); this finding was hypothesized to reflect greater connectivity to or greater dendritic arborization within the striatum due to reduced nigrostriatal projections. Such compensation in XDP might mask the underlying disease process for years before symptoms emerge.

Finally, scenario (4) suggests that genetic alterations in XDP might have changed programming of axon trajectories or pruning to the striatum during development even if neural development within the striatum itself was normal. Such a scenario might manifest as different numbers of projections to one or both striatal compartments, or to a different relative weighting of sensorimotor versus limbic cortex projections between compartments. This fourth possibility is intriguing in that the gene thought to be responsible for XDP (*TAF1*) is involved in modulating apoptosis (Kimura et al., 2008), and because one study previously postulated defects in neurogenesis in XDP brains, based on the finding of alterations in neuropeptide Y immunoreactivity in postmortem tissue (Goto et al., 2013). Indeed, the XDP cohort in the current study showed no relationship between putaminal volume and elevated insula tractography measures, consistent with the hypothesis that tractography abnormalities may have been pre-existing, rather than changing after symptom expression. This leads us to question whether connectivity abnormalities themselves may reflect pathogenesis in XDP, possibly driving degeneration (as hypothesized in (Cyr et al., 2003; Goto et al., 2005; Jakel and Maragos, 2000)), and not just a result of or adaptation to the disease process. Future studies are needed to evaluate

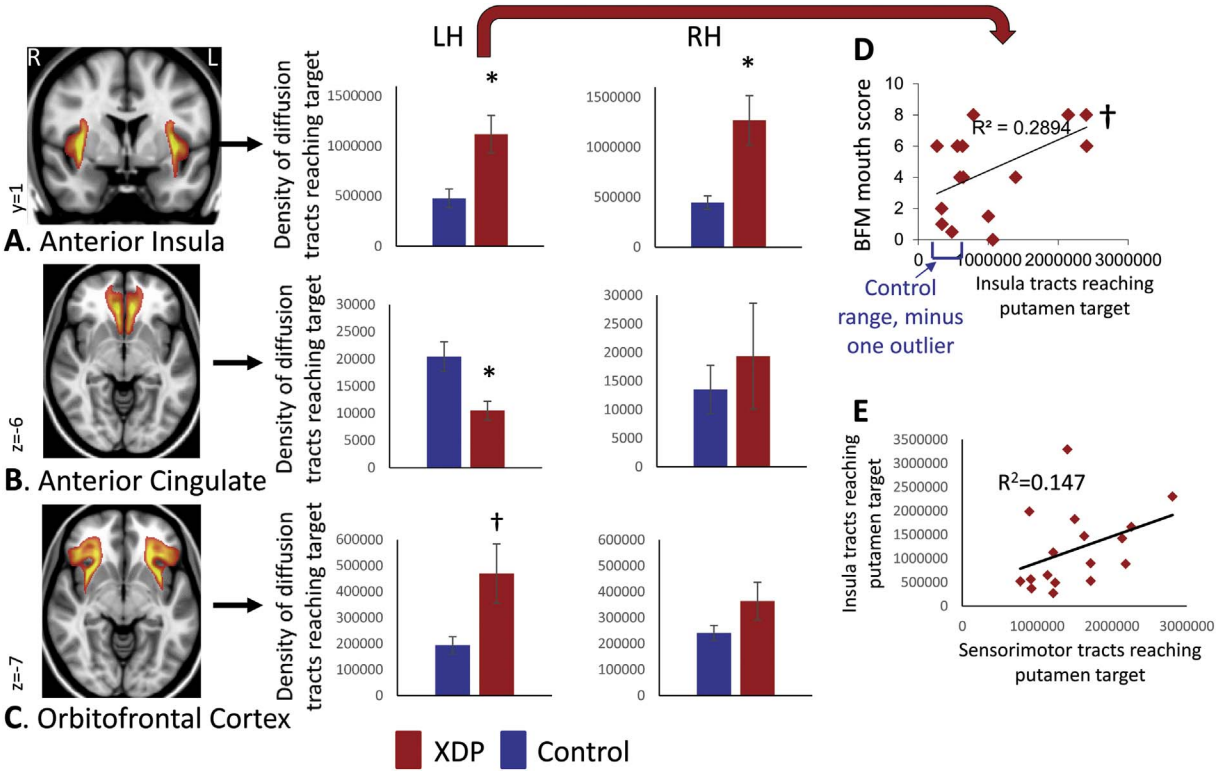

Fig. 3. Comparison of XDP versus control tractography for striosome-weighted connectivity with the putamen (posthoc comparisons). Total termination tractography counts are shown for (A) Anterior Insula, (B), Anterior/subcallosal Cingulate, and (C) Orbitofrontal Cortex connectivity with the left (LH) and right (RH) putamen. Images (from *fslview*) to the left of graphs show representative sections through averaged healthy control tractography maps used in posthoc tractography analyses, superimposed on the MNI152_T1_1mm template. Left and right hemisphere tractography are depicted together in the images, but were evaluated separately for statistics. Note that these images are intended (and thresholded) to be qualitative only, and are included simply to illustrate the territory covered most prominently by each of the measures; they do not convey information about magnitude or spatial extent. *significant at $p < 0.005$; †trend toward significance (within an order of magnitude of the significance p threshold). (D) Relationship between left insula → putamen connectivity and mouth scores on the Burke Fahn Marsden (BFM) scale. (E) Absence of inverse relationship between sensorimotor → putamen and insula → putamen connectivity. XDP: X-linked dystonia-parkinsonism.

Table 6
Striosome-weighted tractography to putamen comparisons for individual regions (10 XDP versus 10 matched controls).

Region	T-test [t (p)]	T-test [t (p)] using ICV-normalized tractography
Left anterior insula to left putamen	2.54 (0.0206)†	2.71 (0.0142)†
Right anterior insula to right putamen	3.16 (0.00540)†	3.63 (0.00190)*
Left anterior/subcallosal cingulate to left putamen	−2.31 (0.0329)†	−2.18 (0.0425)†
Right anterior/subcallosal cingulate to right putamen	0.698 (0.494)	0.779 (0.446)
Left orbitofrontal cortex to left putamen	1.86 (0.0781)†	1.79 (0.0900)†
Right orbitofrontal cortex to right putamen	0.0844 (0.934)	0.194 (0.849)

Positive t values indicate tractography was elevated in XDP patients relative to control subjects; negative t values indicate tractography was reduced in XDP patients relative to control subjects.
XDP: X-linked dystonia-parkinsonism.
ICV: intracranial volume.
* Met significance criteria ($p < 0.005$, [$p < 0.05$, corrected]).
† p value was within an order of magnitude of the corrected threshold (a trend).

young mutation carriers before symptom onset to determine if there is a developmental or prodromal component to this disease.

If we make the assumption that our approach is truly selecting striosome-weighted connectivity, our data suggest that striosomes may show increased, rather than decreased connectivity in XDP. Although the striosome-weighted connectivity with putamen was accompanied most strongly by increased connectivity of the insula with the putamen in XDP, we observed elevated mean connectivity in XDP in every striosome-weighted region except the left anterior cingulate. These differences may drive pathogenesis or may simply relate to pathophysiology; it is not possible to distinguish between these two possibilities in the current study. The results suggest that cell loss in the striosomes may result in connectivity changes and/or that connectivity to striosomes versus matrix develops differently in these individuals. This, in turn, may alter the balance of function in the striatonigral loop normally maintained by the striosomes, leading to excessive function and excitotoxicity over time, as hypothesized in (Cyr et al., 2003; Goto et al., 2005; Jakel and Maragos, 2000). Given that the scanner-matched cohort showed a trend toward reduced matrix-weighted connectivity with putamen in XDP, one scenario might be that increased striosomal connectivity "overdrives" (via the striatonigral loop) a compromised matrix compartment, leading to dystonia until the matrix is so compromised that it is no longer functioning, at which point the symptoms become parkinsonian.

Because our measure of striosome versus matrix connectivity is an indirect one, and because our findings were not what we predicted, alternative hypotheses should be considered regarding interpretation of our findings. The disproportionate increase in insula connectivity suggests the findings may not be as straightforward or compartment-specific as originally anticipated. This may relate to architectural differences in evaluating the different paralimbic regions, or it may suggest there is a particularly important role for the insula in XDP. For example, it is possible that elevated connectivity from insula—and potentially other "striosome-weighted" regions—may have reflected increased matrix, rather than striosome, projections to the putamen. The insula is known to be critical for motor function relating to speech and swallowing [e.g., (Ackermann and Riecker, 2004; Daniels and Foundas,

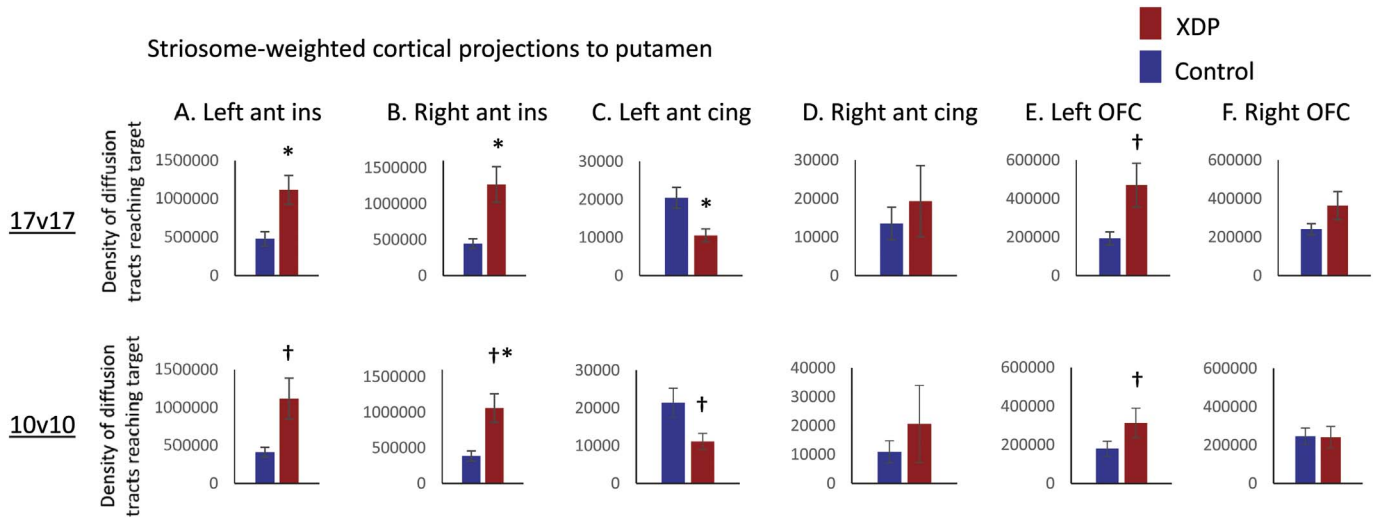

Fig. 4. Comparison of tractography measures for posthoc comparisons in the 17 XDP versus 17 controls cohort, as compared with the 10 XDP versus 10 controls cohort. Total termination tractography counts from Fig. 1 (17 XDP versus 17 controls, top row) are compared with values for the smaller, more tightly matched cohort (bottom row). Individual striosome-weighted regions were individually assessed for connectivity with the ipsilateral putamen: (A) Left anterior insula, (B) Right anterior insula, (C) Left anterior/subcallosal cingulate, (D) Right anterior/subcallosal cingulate, (E) Left orbitofrontal cortex, (F) Right orbitofrontal cortex. Error bars indicate standard error of the mean. *significant at $p < 0.005$; †trend toward significance (within an order of magnitude of the significance p threshold); †* trend without ICV correction, but significant at $p < 0.005$ when ICV corrected. XDP: X-linked dystonia-parkinsonism. ant ins: anterior insula; ant cing: anterior/subcallosal cingulate; OFC: orbitofrontal cortex.

1997; Hamdy et al., 1999; Humbert and McLaren, 2014; Lowell et al., 2012; Martin et al., 2001; Martin et al., 2004; Osawa et al., 2013; Riecker et al., 2009; Zald and Pardo, 1999)]. The insula appears to contribute to individual components of speech and swallowing, in addition to speech and swallowing themselves: insula activation has been observed in humans when tongue, jaw and lip movements are performed independently (Arima et al., 2011; Grabski et al., 2012). Individuals with XDP usually present with severe jaw and tongue dystonia, leading to food intake restriction and an increased risk for aspiration pneumonia (Rosales, 2010). Because of the known role of the insula in these functions, we asked if insula connectivity showed a relationship with speech and mouth dystonia subscores of the BFM, and we found a trend for mouth scores. The large area of the insula included to ask our broader question warrants subparcellation to test for tighter relationships between mouth/speech/swallowing symptoms in XDP. These findings suggest the insula and its connections may offer potential guidance for improving DBS targeting [as used previously for tremor, e.g., (Coenen et al., 2011; Pouratian et al., 2011)], or other treatment for these severely disabling symptoms in XDP.

Whether or not our findings reflect striosome-specificity, we have shown in this study that paralimbic cortical regions show substantial differences in connectivity with the putamen in XDP. This finding is particularly interesting in light of observations of altered gray matter microstructure unique to paralimbic cortices, and not observed in other cortical regions, in a hypothesized biological subtype of major depressive disorder (Blood et al., 2010). This raises the question whether paralimbic cortex might be more plastic, more vulnerable, and/or subjected to different genetic or environmental regulation than other cortical regions, a factor that may prove critical to our mechanistic understanding of diseases affecting the limbic/paralimbic circuitry.

The left anterior/subcallosal cingulate was the only paralimbic region that showed reduced connectivity with the putamen. This finding is of interest both (1) with regard to a potential role in comorbid symptoms of depression and anxiety in XDP (Jamora et al., 2014; Morigaki et al., 2013) and (2) with regard to the cingulate's role in motivational akinesia and mutism (Fix, 2008). It is thus worth considering that some of the bradykinesia and speech difficulties in XDP arise from a limbic/motivational, as well as a purely motor origin. There was an absence of tractography correlations with the majority of clinical indices evaluated in the XDP cohort, including duration, overall symptom severity, and depression/anxiety scores. This finding is consistent with the heterogeneity of clinical observations and course of the disease, suggesting that substantially larger cohorts are needed to assess the relationship of imaging to specific clinical variables in XDP. However, the absence of strong relationships to clinical variables may also reflect the "blunt" approach designed for the high-level, data-driven approach used in the current study. Specifically, to achieve the goals of this study, tractography was run for entire regions (e.g., entire insula, entire putamen), and was not designed to be specific to any single clinical output measure. Voxelwise studies using clinical variables as covariates may be more likely to identify such relationships. In addition, clinical variables paired with tractography may be clinically useful, but are not defined based on a specific neural substrate, and likely reflect changes at more than one site or tract.

4.1. Limitations

As with all imaging studies, there are certain limitations to the findings in this study that should be considered.

First, we optimized our cohort matching despite the magnet change late in data acquisition. Given the findings were similar in a smaller cohort all scanned in the same magnet, we feel confident the findings are robust. Although the lower statistical power in the smaller cohort led to reduced statistical significance, the right insula finding was indeed significant for this cohort when corrected for ICV. Nevertheless, studies in larger cohorts will be important to show our findings replicate, and to determine if our findings represent a more general paralimbic effect or an effect specific to the insula.

Second, limited availability of HADS scores made it difficult to be certain if the absence of their relationship to tractography measures reflected true negatives versus insufficient power to detect an effect. Future studies should also evaluate these measures in larger cohorts.

Third, tractography between structures as close as the insula and the putamen appears more prone to sporadic effects not related to connectivity, and thus should be interpreted with caution (Gigandet et al., 2008). We aimed to account for distance factors by using the distance correction in the FDT toolbox for all of our tractography data; however, there may be non-linear effects of short distances in small, high traffic regions, such as the external capsule. In addition, use of termination, rather than waypoint, tractography in this study was used to minimize

any impact of atrophy within the striatum on tractography measures, and there was no linear relationship between degree of putaminal atrophy (i.e., putamen volume) and insula tractography in XDP. However, there remains a possibility that striatal atrophy in the XDP group also influenced tractography measures in this study independent of true connectivity metrics.

Fourth, we cannot assume there is a one-to-one correlation of lost striatal tissue and reduction in afferents to this tissue. Since we cannot make direct measures of tissue in vivo, we also cannot be certain that our measures are striosome- versus matrix-specific. Therefore a direct interpretation of our findings in relation to the precise shift in striosome/matrix ratio is not possible here. Nevertheless, the changes in afferents do indeed support the premise of altered circuitry in XDP, including the likelihood of a shift in the balance of striosome to matrix afferents, whether from early development or secondary to neuronal loss in the striatum.

Fifth, we studied patients with short disease durations of one to six years who were predominantly in the dystonic phase of XDP. Future studies should include patients in temporally more advanced disease stages, i.e. the parkinsonian phase, who are thought to have a stronger involvement of striatal matrix. In addition, it is clear that studies of presymptomatic individuals must be conducted to determine the extent to which altered connectivity (and/or volume reduction) is present in years prior to symptom onset.

5. Conclusions

In the current study, we aimed to add to the sparse in vivo literature on the pathology and pathophysiology of XDP. Based on the hypothesis that striosomes degenerate earlier than matrix in individuals with XDP, we evaluated whether connectivity to striosome-weighted versus matrix-weighted regions was altered in these individuals. Rather than finding greater reductions in striosome-weighted afferent connectivity, we found paradoxical elevation in striosome-weighted connectivity to the putamen, driven primarily by the anterior insula. While this approach did not provide a straightforward answer to our original hypothesis, the results suggest that cell loss in the striatum may result in reorganization and/or that striatal connectivity develops or is regulated differently in these individuals. The observation of increased insula connectivity is intriguing given that XDP typically presents with significant jaw and tongue dystonia. The role of the insula in XDP pathophysiology should be further investigated to determine its potential application toward treatment of these disabling symptoms.

Supplementary data to this article can be found online at https://doi.org/10.1016/j.nicl.2017.10.025.

Acknowledgments

We wish to thank the scientific members of the Collaborative Center for X-linked Dystonia-Parkinsonism (XDP) at Massachusetts General Hospital who participated in the 2014 and 2015 Annual CCXDP workshop. These individuals provided valuable discussion and background information that facilitated conception and development of the questions tested in the current study. In particular, discussions in these workshops raised the question whether further study of putative striatal compartment disparities in XDP (i.e., earlier degeneration of striosomes than matrix) would give us clues to disease mechanism.

The authors also thank Myung Joo Lee for her assistance with demographic matching statistics.

Funding

This study was funded by University Hospital Schleswig-Holstein, the University of Lübeck, the German Research Foundation (CRC936), and the Collaborative Center for X-linked Dystonia-Parkinsonism (XDP) at Massachusetts General Hospital. CK is the recipient of a career development award from the Hermann and Lilly Schilling Foundation.

References

Ackermann, H., Riecker, A., 2004. The contribution of the insula to motor aspects of speech production: a review and a hypothesis. Brain Lang. 89, 320–328.
Argyelan, M., Carbon, M., Niethammer, M., Ulug, A.M., Voss, H.U., Bressman, S.B., Dhawan, V., Eidelberg, D., 2009. Cerebellothalamocortical connectivity regulates penetrance in dystonia. J. Neurosci. 29, 9740–9747.
Arima, T., Yanagi, Y., Niddam, D.M., Ohata, N., Arendt-Nielsen, L., Minagi, S., Sessle, B.J., Svensson, P., 2011. Corticomotor plasticity induced by tongue-task training in humans: a longitudinal fMRI study. Exp. Brain Res. 212, 199–212.
Arndt, S., Cohen, G., Alliger, R.J., Swayze 2nd, V.W., Andreasen, N.C., 1991. Problems with ratio and proportion measures of imaged cerebral structures. Psychiatry Res. 40, 79–89.
Beaulieu, C., 2002. The basis of anisotropic water diffusion in the nervous system — a technical review. NMR Biomed. 15, 435–455.
Behrens, T.E., Berg, H.J., Jbabdi, S., Rushworth, M.F., Woolrich, M.W., 2007. Probabilistic diffusion tractography with multiple fibre orientations: what can we gain? NeuroImage 34, 144–155.
Beste, C., Baune, B.T., Domschke, K., Falkenstein, M., Konrad, C., 2010. Dissociable influences of NR2B-receptor related neural transmission on functions of distinct associative basal ganglia circuits. NeuroImage 52, 309–315.
Binkofski, F., Reetz, K., Gaser, C., Hilker, R., Hagenah, J., Hedrich, K., van Eimeren, T., Thiel, A., Buchel, C., Pramstaller, P.P., Siebner, H.R., Klein, C., 2007. Morphometric fingerprint of asymptomatic Parkin and PINK1 mutation carriers in the basal ganglia. Neurology 69, 842–850.
Blood, A.J., Tuch, D.S., Makris, N., Makhlouf, M.L., Sudarsky, L.R., Sharma, N., 2006. White matter abnormalities in dystonia normalize after botulinum toxin treatment. Neuroreport 17, 1251–1255.
Blood, A.J., Iosifescu, D.V., Makris, N., Perlis, R.H., Kennedy, D.N., Dougherty, D.D., Kim, B.W., Lee, M.J., Wu, S., Lee, S., Calhoun, J., Hodge, S.M., Fava, M., Rosen, B.R., Smoller, J.W., Gasic, G.P., Breiter, H.C., 2010. Microstructural abnormalities in subcortical reward circuitry of subjects with major depressive disorder. PLoS One 5, e13945.
Blood, A.J., Kuster, J.K., Woodman, S.C., Kirlic, N., Makhlouf, M.L., Multhaupt-Buell, T.J., Makris, N., Parent, M., Sudarsky, L.R., Sjalander, G., Breiter, H., Breiter, H.C., Sharma, N., 2012. Evidence for altered Basal Ganglia-brainstem connections in cervical dystonia. PLoS One 7, e31654.
Breiter, H.C., Filipek, P.A., Kennedy, D.N., Baer, L., Pitcher, D.A., Olivares, M.J., Renshaw, P.F., Caviness Jr., V.S., 1994. Retrocallosal white matter abnormalities in patients with obsessive-compulsive disorder. Arch. Gen. Psychiatry 51, 663–664.
Bruggemann, N., Heldmann, M., Klein, C., Domingo, A., Rasche, D., Tronnier, V., Rosales, R.L., Jamora, R.D., Lee, L.V., Munte, T.F., 2016. Neuroanatomical changes extend beyond striatal atrophy in X-linked dystonia parkinsonism. Parkinsonism Relat. Disord. 31, 91–97.
Bruggemann, N., Rosales, R.L., Waugh, J.L., Blood, A.J., Domingo, A., Heldmann, M., Jamora, R.D., Munchau, A., Munte, T.F., Lee, L.V., Buchmann, I., Klein, C., 2017. Striatal dysfunction in X-linked dystonia-parkinsonism is associated with disease progression. Eur. J. Neurol. 24, 680–686.
Carbon, M., Kingsley, P.B., Su, S., Smith, G.S., Spetsieris, P., Bressman, S., Eidelberg, D., 2004. Microstructural white matter changes in carriers of the DYT1 gene mutation. Ann. Neurol. 56, 283–286.
Chouinard, P.A., Paus, T., 2006. The primary motor and premotor areas of the human cerebral cortex. Neuroscientist 12, 143–152.
Coenen, V.A., Allert, N., Madler, B., 2011. A role of diffusion tensor imaging fiber tracking in deep brain stimulation surgery: DBS of the dentato-rubro-thalamic tract (drt) for the treatment of therapy-refractory tremor. Acta Neurochir. 153, 1579–1585 (discussion 1585).
Crittenden, J.R., Graybiel, A.M., 2011. Basal Ganglia disorders associated with imbalances in the striatal striosome and matrix compartments. Front. Neuroanat. 5, 59.
Cyr, M., Beaulieu, J.M., Laakso, A., Sotnikova, T.D., Yao, W.D., Bohn, L.M., Gainetdinov, R.R., Caron, M.G., 2003. Sustained elevation of extracellular dopamine causes motor dysfunction and selective degeneration of striatal GABAergic neurons. Proc. Natl. Acad. Sci. U. S. A. 100, 11035–11040.
Daniels, S.K., Foundas, A.L., 1997. The role of the insular cortex in dysphagia. Dysphagia 12, 146–156.
Delmaire, C., Vidailhet, M., Wassermann, D., Descoteaux, M., Valabregue, R., Bourdain, F., Lenglet, C., Sangla, S., Terrier, A., Deriche, R., Lehericy, S., 2009. Diffusion abnormalities in the primary sensorimotor pathways in writer's cramp. Arch. Neurol. 66, 502–508.
Domingo, A., Westenberger, A., Lee, L.V., Braenne, I., Liu, T., Vater, I., Rosales, R., Jamora, R.D., Pasco, P.M., Cutiongco-Dela Paz, E.M., Freimann, K., Schmidt, T.G., Dressler, D., Kaiser, F.J., Bertram, L., Erdmann, J., Lohmann, K., Klein, C., 2015. New insights into the genetics of X-linked dystonia-parkinsonism (XDP, DYT3). Eur. J. Hum. Genet. 23, 1334–1340.
Dure, L.S.t., Young, A.B., Penney Jr., J.B., 1992. Compartmentalization of excitatory amino acid receptors in human striatum. Proc. Natl. Acad. Sci. U. S. A. 89, 7688–7692.
Eblen, F., Graybiel, A.M., 1995. Highly restricted origin of prefrontal cortical inputs to striosomes in the macaque monkey. J. Neurosci. 15, 5999–6013.
Eidelberg, D., Takikawa, S., Wilhelmsen, K., Dhawan, V., Chaly, T., Robeson, W., Dahl, R., Margouleff, D., Greene, P., Hunt, A., et al., 1993. Positron emission tomographic findings in Filipino X-linked dystonia-parkinsonism. Ann. Neurol. 34, 185–191.
Engvig, A., Fjell, A.M., Westlye, L.T., Moberget, T., Sundseth, O., Larsen, V.A., Walhovd,

K.B., 2012. Memory training impacts short-term changes in aging white matter: a longitudinal diffusion tensor imaging study. Hum. Brain Mapp. 33, 2390–2406.
Fix, J., 2008. High-Yield Neuroanatomy, 4th ed. Lippincott Williams & Wilkins, Philadelphia.
Friedman, A., Homma, D., Gibb, L.G., Amemori, K., Rubin, S.J., Hood, A.S., Riad, M.H., Graybiel, A.M., 2015. A corticostriatal path targeting striosomes controls decision-making under conflict. Cell 161, 1320–1333.
Gasic, G.P., Smoller, J.W., Perlis, R.H., Sun, M., Lee, S., Kim, B.W., Lee, M.J., Holt, D.J., Blood, A.J., Makris, N., Kennedy, D.K., Hoge, R.D., Calhoun, J., Fava, M., Gusella, J.F., Breiter, H.C., 2009. BDNF, relative preference, and reward circuitry responses to emotional communication. Am. J. Med. Genet. B Neuropsychiatr. Genet. 150B, 762–781.
Gerfen, C.R., 1984. The neostriatal mosaic: compartmentalization of corticostriatal input and striatonigral output systems. Nature 311, 461–464.
Gerfen, C.R., 1989. The neostriatal mosaic: striatal patch-matrix organization is related to cortical lamination. Science 246, 385–388.
Gigandet, X., Hagmann, P., Kurant, M., Cammoun, L., Meuli, R., Thiran, J.P., 2008. Estimating the confidence level of white matter connections obtained with MRI tractography. PLoS One 3, e4006.
Goto, S., Lee, L.V., Munoz, E.L., Tooyama, I., Tamiya, G., Makino, S., Ando, S., Dantes, M.B., Yamada, K., Matsumoto, S., Shimazu, H., Kuratsu, J., Hirano, A., Kaji, R., 2005. Functional anatomy of the basal ganglia in X-linked recessive dystonia-parkinsonism. Ann. Neurol. 58, 7–17.
Goto, S., Kawarai, T., Morigaki, R., Okita, S., Koizumi, H., Nagahiro, S., Munoz, E.L., Lee, L.V., Kaji, R., 2013. Defects in the striatal neuropeptide Y system in X-linked dystonia-parkinsonism. Brain 136, 1555–1567.
Grabski, K., Lamalle, L., Vilain, C., Schwartz, J.L., Vallee, N., Tropres, I., Baciu, M., Le Bas, J.F., Sato, M., 2012. Functional MRI assessment of orofacial articulators: neural correlates of lip, jaw, larynx, and tongue movements. Hum. Brain Mapp. 33, 2306–2321.
Graybiel, A.M., Canales, J.J., Capper-Loup, C., 2000. Levodopa-induced dyskinesias and dopamine-dependent stereotypies: a new hypothesis. Trends Neurosci. 23, S71–77.
Hamdy, S., Rothwell, J.C., Brooks, D.J., Bailey, D., Aziz, Q., Thompson, D.G., 1999. Identification of the cerebral loci processing human swallowing with H2(15)O PET activation. J. Neurophysiol. 81, 1917–1926.
Hess, C.W., Ofori, E., Akbar, U., Okun, M.S., Vaillancourt, D.E., 2013. The evolving role of diffusion magnetic resonance imaging in movement disorders. Curr. Neurol. Neurosci. Rep. 13, 400.
Humbert, I.A., McLaren, D.G., 2014. Differential psychophysiological interactions of insular subdivisions during varied oropharyngeal swallowing tasks. Phys. Rep. 2, e00239.
Isacson, O., Sofroniew, M.V., 1992. Neuronal loss or replacement in the injured adult cerebral neocortex induces extensive remodeling of intrinsic and afferent neural systems. Exp. Neurol. 117, 151–175.
Jakel, R.J., Maragos, W.F., 2000. Neuronal cell death in Huntington's disease: a potential role for dopamine. Trends Neurosci. 23, 239–245.
Jamora, R.D., Ledesma, L.K., Domingo, A., Cenina, A.R., Lee, L.V., 2014. Nonmotor features in sex-linked dystonia parkinsonism. Neurodegener. Dis. Manag. 4, 283–289.
Jimenez-Castellanos, J., Graybiel, A.M., 1987. Subdivisions of the dopamine-containing A8-A9-A10 complex identified by their differential mesostriatal innervation of striosomes and extrastriosomal matrix. Neuroscience 23, 223–242.
Kimura, J., Nguyen, S.T., Liu, H., Taira, N., Miki, Y., Yoshida, K., 2008. A functional genome-wide RNAi screen identifies TAF1 as a regulator for apoptosis in response to genotoxic stress. Nucleic Acids Res. 36, 5250–5259.
Kincaid, A.E., Wilson, C.J., 1996. Corticostriatal innervation of the patch and matrix in the rat neostriatum. J. Comp. Neurol. 374, 578–592.
Langer, L.F., Graybiel, A.M., 1989. Distinct nigrostriatal projection systems innervate striosomes and matrix in the primate striatum. Brain Res. 498, 344–350.
Lee, L.V., Munoz, E.L., Tan, K.T., Reyes, M.T., 2001. Sex linked recessive dystonia parkinsonism of Panay, Philippines (XDP). Mol. Pathol. 54, 362–368.
Lee, L.V., Rivera, C., Teleg, R.A., Dantes, M.B., Pasco, P.M., Jamora, R.D., Arancillo, J., Villareal-Jordan, R.F., Rosales, R.L., Demaisip, C., Maranon, E., Peralta, O., Borres, R., Tolentino, C., Monding, M.J., Sarcia, S., 2011. The unique phenomenology of sex-linked dystonia parkinsonism (XDP, DYT3, “Lubag”). Int. J. Neurosci. 121 (Suppl. 1), 3–11.
Lovden, M., Bodammer, N.C., Kuhn, S., Kaufmann, J., Schutze, H., Tempelmann, C., Heinze, H.J., Duzel, E., Schmiedek, F., Lindenberger, U., 2010. Experience-dependent plasticity of white-matter microstructure extends into old age. Neuropsychologia 48, 3878–3883.
Lowell, S.Y., Reynolds, R.C., Chen, G., Horwitz, B., Ludlow, C.L., 2012. Functional connectivity and laterality of the motor and sensory components in the volitional swallowing network. Exp. Brain Res. 219, 85–96.
Makino, S., Kaji, R., Ando, S., Tomizawa, M., Yasuno, K., Goto, S., Matsumoto, S., Tabuena, M.D., Maranon, E., Dantes, M., Lee, L.V., Ogasawara, K., Tooyama, I., Akatsu, H., Nishimura, M., Tamiya, G., 2007. Reduced neuron-specific expression of the TAF1 gene is associated with X-linked dystonia-parkinsonism. Am. J. Hum. Genet. 80, 393–406.
Makris, N., Gasic, G.P., Kennedy, D.N., Hodge, S.M., Kaiser, J.R., Lee, M.J., Kim, B.W., Blood, A.J., Evins, A.E., Seidman, L.J., Iosifescu, D.V., Lee, S., Baxter, C., Perlis, R.H., Smoller, J.W., Fava, M., Breiter, H.C., 2008. Cortical thickness abnormalities in cocaine addiction—a reflection of both drug use and a pre-existing disposition to drug abuse? Neuron 60, 174–188.
Martin, R.E., Goodyear, B.G., Gati, J.S., Menon, R.S., 2001. Cerebral cortical representation of automatic and volitional swallowing in humans. J. Neurophysiol. 85, 938–950.
Martin, R.E., MacIntosh, B.J., Smith, R.C., Barr, A.M., Stevens, T.K., Gati, J.S., Menon, R.S., 2004. Cerebral areas processing swallowing and tongue movement are overlapping but distinct: a functional magnetic resonance imaging study. J. Neurophysiol. 92, 2428–2443.
Morigaki, R., Nakataki, M., Kawarai, T., Lee, L.V., Teleg, R.A., Tabuena, M.D., Mure, H., Sako, W., Pasco, P.M., Nagahiro, S., Iga, J., Ohmori, T., Goto, S., Kaji, R., 2013. Depression in X-linked dystonia-parkinsonism: a case-control study. Parkinsonism Relat. Disord. 19, 844–846.
Murray, R.C., Logan, M.C., Horner, K.A., 2015. Striatal patch compartment lesions reduce stereotypy following repeated cocaine administration. Brain Res. 1618, 286–298.
Nolte, D., Niemann, S., Muller, U., 2003. Specific sequence changes in multiple transcript system DYT3 are associated with X-linked dystonia parkinsonism. Proc. Natl. Acad. Sci. U. S. A. 100, 10347–10352.
Osawa, A., Maeshima, S., Matsuda, H., Tanahashi, N., 2013. Functional lesions in dysphagia due to acute stroke: discordance between abnormal findings of bedside swallowing assessment and aspiration on videofluorography. Neuroradiology 55, 413–421.
Picard, N., Strick, P.L., 2001. Imaging the premotor areas. Curr. Opin. Neurobiol. 11, 663–672.
Pouratian, N., Zheng, Z., Bari, A.A., Behnke, E., Elias, W.J., Desalles, A.A., 2011. Multi-institutional evaluation of deep brain stimulation targeting using probabilistic connectivity-based thalamic segmentation. J. Neurosurg. 115, 995–1004.
Ragsdale Jr., C.W., Graybiel, A.M., 1981. The fronto-striatal projection in the cat and monkey and its relationship to inhomogeneities established by acetylcholinesterase histochemistry. Brain Res. 208, 259–266.
Riecker, A., Gastl, R., Kuhnlein, P., Kassubek, J., Prosiegel, M., 2009. Dysphagia due to unilateral infarction in the vascular territory of the anterior insula. Dysphagia 24, 114–118.
Rosales, R.L., 2010. X-linked dystonia parkinsonism: clinical phenotype, genetics and therapeutics. J Mov Disord 3, 32–38.
Scholz, J., Klein, M.C., Behrens, T.E., Johansen-Berg, H., 2009. Training induces changes in white-matter architecture. Nat. Neurosci. 12, 1370–1371.
Taljan, K., McIntyre, C., Sakaie, K., 2011. Anatomical connectivity between subcortical structures. Brain Connect. 1, 111–118.
Ullen, F., 2009. Is activity regulation of late myelination a plastic mechanism in the human nervous system? Neuron Glia Biol. 5, 29–34.
Voevodskaya, O., Simmons, A., Nordenskjold, R., Kullberg, J., Ahlstrom, H., Lind, L., Wahlund, L.O., Larsson, E.M., Westman, E., 2014. The effects of intracranial volume adjustment approaches on multiple regional MRI volumes in healthy aging and Alzheimer's disease. Front. Aging Neurosci. 6, 264.
Waters, C.H., Faust, P.L., Powers, J., Vinters, H., Moskowitz, C., Nygaard, T., Hunt, A.L., Fahn, S., 1993. Neuropathology of lubag (x-linked dystonia parkinsonism). Mov. Disord. 8, 387–390.
Waugh, J.L., Kuster, J.K., Levenstein, J.M., Makris, N., Multhaupt-Buell, T.J., Sudarsky, L.R., Breiter, H.C., Sharma, N., Blood, A.J., 2016. Thalamic volume is reduced in cervical and laryngeal dystonias. PLoS One 11, e0155302.
White, L.E., Andrews, T.J., Hulette, C., Richards, A., Groelle, M., Paydarfar, J., Purves, D., 1997. Structure of the human sensorimotor system. I: morphology and cytoarchitecture of the central sulcus. Cereb. Cortex 7, 18–30.
Yakovlev, P., Lecours, A., 1982. The myelogenetic cycles of neuronal maturation of the brain. In: Histopathology of the Nervous System. Charles C Thomas Publisher, Springfield, IL, pp. 3–70.
Zald, D.H., Pardo, J.V., 1999. The functional neuroanatomy of voluntary swallowing. Ann. Neurol. 46, 281–286.